Available online at www.sciencedirect.com
ScienceDirect
Trans. Nonferrous Met. Soc. China 21(2011) 109−113
Transactions of Nonferrous Metals Society of China
www.tnmsc.cn

Microstructure and magnetic properties of Ni-Zn ferrites doped with MnO_2

SU Hua, ZHANG Huai-wu, TANG Xiao-li, JING Yu-lan

State Key Laboratory of Electronic Thin Films and Integrated Devices,
University of Electronic Science and Technology of China, Chengdu 610054, China

Received 15 March 2010; accepted 28 May 2010

Abstract: To improve the performance of Ni-Zn ferrites for power field use, the influence of MnO_2 additive on the properties of Ni-Zn ferrites was investigated by the conventional powder metallurgy. The results show that MnO_2 does not form a visible second phase in the doping mass fraction range of (0−2.0%). The average grain size, sintering density and real permeability gradually decrease with the increase of the MnO_2 content. And the DC resistivity continuously increases with the increase of MnO_2 content. The saturation magnetization (magnetic moment in unit mass) first increases slightly when mass fraction of MnO_2 is less than 0.4% MnO_2, and then gradually decreases with increasing the MnO_2 mass fraction due to the exchange interaction of the cations. When the excitation frequency is less than 1 MHz, the power loss (P_{cv}) continuously increases with increasing the MnO_2 content due to the decrease of average grain size. However, when the excitation frequency exceeds 1 MHz, eddy current loss gradually becomes the predominant contribution to P_{cv}. And the sample with a higher resistivity favors a lower P_{cv}, except for the sample with 2.0% MnO_2. The sample without additive has the best P_{cv} when worked at frequencies less than 1 MHz; and the sample with 1.6% MnO_2 additive has the best P_{cv} when worked at frequencies higher than 1 MHz.
Key words: Ni-Zn ferrite; MnO_2; doping; magnetic properties

1 Introduction

Recently, with the downsizing of various electronic components, the power transformers, inductors, choke coils and other electromagnetic components are required to work at higher frequency. Polycrystalline Ni-Zn ferrites find their utility for power applications at frequency over 1 MHz because they have many attractive characteristics for high frequency usage, such as high electrical resistivity, high cut-off frequency and chemical stability[1−4]. The electromagnetic properties of Ni-Zn ferrites have been investigated by many researchers[5−8], and many additives, such as V_2O_5/Nb_2O_5, B_2O_3 and Co_2O_3, have been introduced into Ni-Zn ferrites to improve some magnetic properties[9−11]. However, researches on Ni-Zn ferrites for power field use are less. Important requirements for this kind of Ni-Zn ferrites are the high saturation magnetization and low core loss. Saturation magnetization of the spinel ferrites is mainly determined by their compositions; however, core loss of the ferrites is also very sensitive to the microstructure, impurity species and levels. In this work, the composition of the Ni-Zn ferrites was fixed as $Ni_{0.7}Zn_{0.3}Fe_2O_4$, which presented a relatively high saturation magnetization and cut-off frequency, and the effects of MnO_2 additive on the microstructure, sintering density and magnetic properties of the Ni-Zn ferrites were investigated to improve the performance of Ni-Zn ferrites for power field use.

2 Experimental

The conventional ceramic processing was used to prepare the samples. First, the raw materials (Fe_2O_3, ZnO, NiO) were weighed in stoichiometric proportions and wet-mixed for 4 h in a ball mill. After drying, the mixtures were calcined at 1 000 ºC for 2 h in air. Then the calcined powders were mixed with a prescribed amount of MnO_2 ranging from 0.0 to 2.0% (mass fraction) in step of 0.4% and each wet-milled for 6 h in planetary mills. Following the addition of polyvinyl alcohols (PVA), the milled powders were granulated and pressed into toroidal and disk shapes, which were finally sintered at 1 230 °C for 3 h in air and left to cool inside

Foundation item: Projects(50702011, 60721001) supported by the National Natural Science Foundation of China
Corresponding author: SU Hua; Tel: +86-28-83203793; Fax: +86-28-83201810; E-mail: uestcsh@163.com
DOI: 10.1016/S1003-6326(11)60685-7

the electric furnace.

The phases were identified by X-ray diffractometry using Cu K_α radiation. Micrographs were taken on a scanning electron microscope (SEM). The sintering density was calculated as the mass/volume ratio. The saturation magnetization was measured on a vibrating sample magnetometer (VSM, BHV−525). The DC resistivity (ρ) at room temperature was measured by the bridge method with silver paste contacts. The permeability spectrum was measured on a RF impedance analyzer (HP4291B) within the frequency range of 1 MHz−1 GHz. The core loss was measured on a B-H analyzer (IWATSU, SY−8232) at room temperature.

3 Results and discussion

The XRD patterns of samples without and with 2.0% MnO_2 are shown in Fig.1. A single phase spinel structure is observed for the two samples, which means that MnO_2 additive does not form a visible second phase in the tested samples.

Fig.2 shows SEM images of samples with different MnO_2 contents. The average grain size gradually decreases from 4−6 μm for the undoped sample to approximately 1−1.5 μm for the sample doped with 2.0% MnO_2. Furthermore, MnO_2 is in favor of restraining

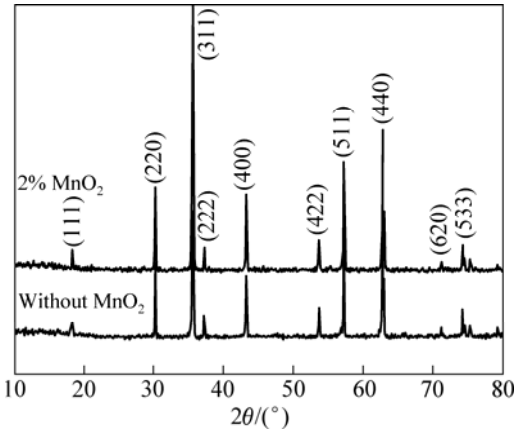

Fig.1 XRD patterns of Ni-Zn ferrites without and with 2.0% MnO_2

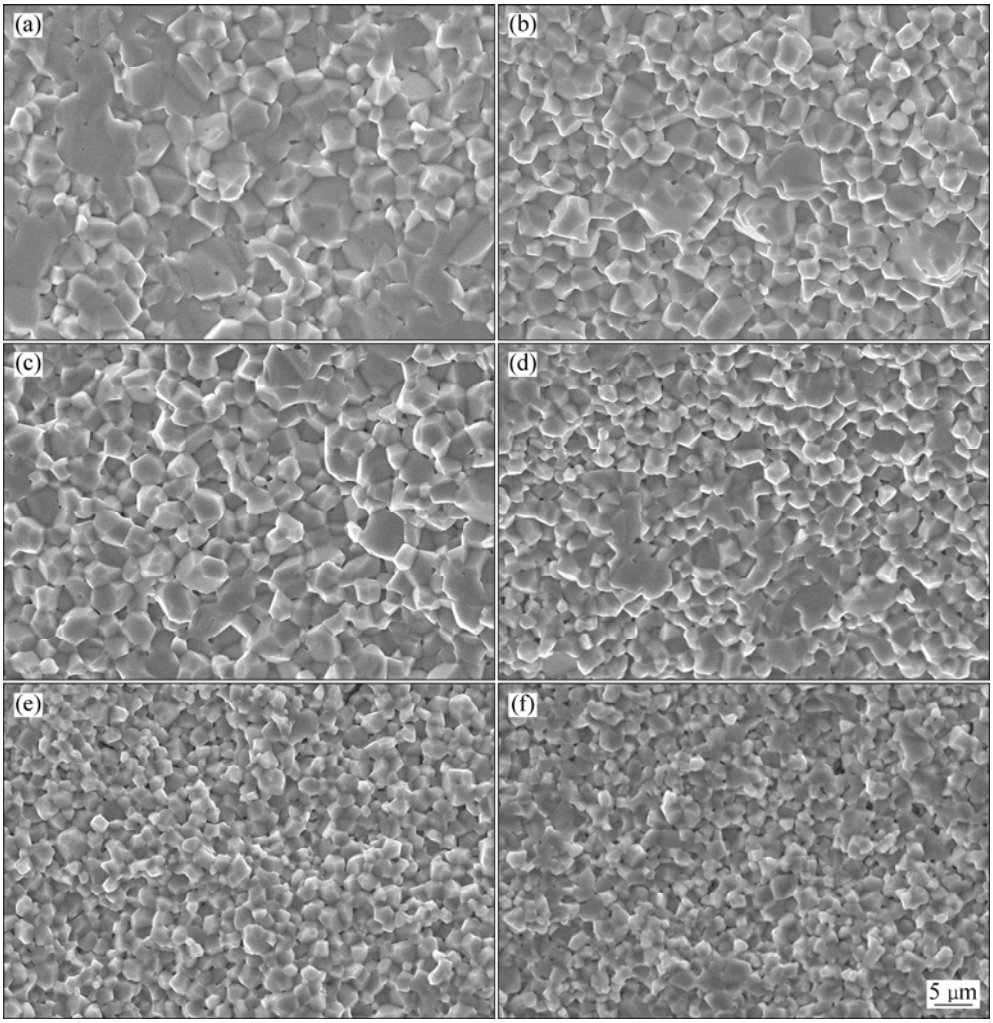

Fig.2 SEM images of Ni-Zn ferrites with different MnO_2 mass fractions: (a) Without MnO_2; (b) 0.4% MnO_2; (c) 0.8% MnO_2; (d) 1.2% MnO_2; (e) 1.6% MnO_2; (f) 2.0% MnO_2

abnormal grain growth.

Table1 shows the variations in sintering density, saturation magnetization (1 kA/m=1 emu/g) and DC resistivity with MnO_2 content. MnO_2 prevents grain growth, which leads to the continuous decrease of sintering density. The saturation magnetization has first a slight increase, and then decreases with increasing MnO_2 content. Due to the saturation magnetization being the magnetic moment in unit mass, it is not influenced by sintering density. And the variation could be explained on the basis of cation distribution and exchange interaction between iron and manganese ions at tetrahedral (A) and octahedral (B) sites. It is known that Zn^{2+} and Ni^{2+} ions occupy A and B sites, respectively. Although iron and manganese ions exist at both A and B sites, they have preference for the B and A sites. respectively[12]. When manganese ions are introduced into the ferrite samples, they prefer to occupy A sites, which leads to some iron ions migrating from A to B sites and increases magnetic moment of B sublattice. Furthermore, although the magnetic moment of Mn^{2+} is the same as that of Fe^{3+} (5 μB), the exchange interaction between manganese and iron ions is small. And there will be canting of spins of Fe^{3+} and Mn^{2+} ions at the A sites, which leads to decreasing the magnetic moment of A sublattice[12]. So, the molecular magnetic moment of the ferrite, which equals the balance of the B and A sublattices' magnetic moment, increases with the MnO_2 content first. However, when the mass fraction of MnO_2 exceeds 0.4%, the saturation magnetization exhibits a slight decrease. This may be attributed to the fact that some Mn^{3+} ions appear in the ferrites and weaken the magnetic moment of B sublattice. Furthermore, microstructure also has a slight influence on saturation magnetization. A smaller average grain size favors a lower saturation magnetization. MnO_2 additive leads to the decrease of average grain size and favors the decrease of saturation magnetization. The DC resistivity continuously increases with increasing MnO_2 content. It is known that the dominant conduction mechanism in spinel ferrites is an electron exchange between Fe^{2+} and Fe^{3+} ions on octahedral sites. The occurrence of Mn^{3+} ions during the slow cooling can decrease Fe^{2+} concentration by following reaction[13]:

$$Fe^{2+} + Mn^{3+} \rightarrow Fe^{3+} + Mn^{2+}$$

and the n-type conduction generated by ferrous ions diminishes. Also, the p-type conduction will be eliminated by Mn^{2+} ions that have a smaller ionization energy (34.2 eV) than Ni^{2+} (36.1 eV) oxidized by following reaction[13−14]:

$$Ni^{3+} + Mn^{2+} \rightarrow Ni^{2+} + Mn^{3+}$$

Furthermore, the decrease of sintering density and average grain size also favor the increase of resistivity. As a result, the DC resistivity gradually increases with the increase of MnO_2 content.

Fig.3 shows the permeability values of samples. Permeability gradually decreases with increasing MnO_2 content. This fact is attributed mainly to the decrease of average grain size and sintering density. Fig.4 shows the dependence of frequency on power loss for the samples under the induction flux density of 5 mT.

Table 1 Sintering density, saturation magnetization and DC resistivity of samples

Sample	Sintering density/ ($g \cdot cm^{-3}$)	Saturation magnetization/ ($kA \cdot m^{-1}$)	DC resistivity/ ($\Omega \cdot cm^{-1}$)
Without MnO_2	5.142−5.154	71.5	8.44×10^5
0.4% MnO_2	5.116−5.128	72.3	1.81×10^6
0.8% MnO_2	5.045−5.057	71.6	7.72×10^6
1.2% MnO_2	4.966−4.978	70.5	1.95×10^7
1.6% MnO_2	4.908−4.920	69.7	5.21×10^7
2.0% MnO_2	4.824−4.836	68.7	8.86×10^7

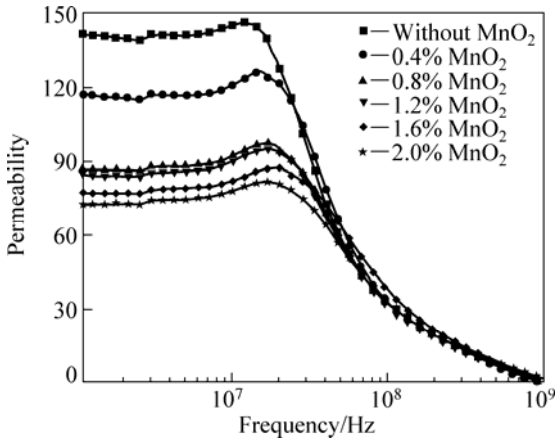

Fig.3 Permeability values of samples with different MnO_2 mass fractions

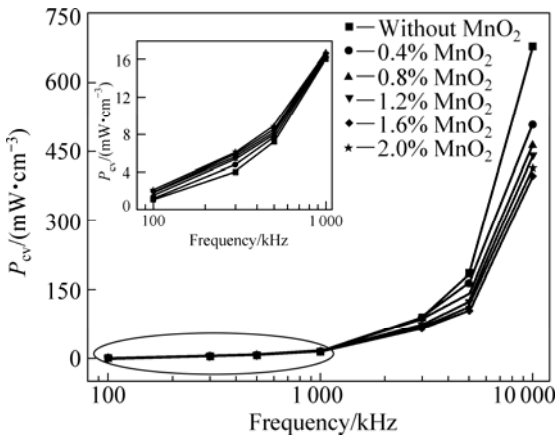

Fig.4 Dependence of frequency on power low (P_{cv}) under induction flux density of 5 mT

When the excitation frequency is less than 1 MHz, the sample with a less MnO_2 content and bigger average grain size obtains a lower P_{cv}. However, when the excitation frequency is higher than 1 MHz, the sample with a higher MnO_2 content and smaller average grain size obtains a lower P_{cv}, except for the sample with the maximum MnO_2 content. It is known that the P_{cv} of ferrite materials can be divided into hysteresis loss (P_h), eddy current loss (P_e) and residual loss (P_r). Since Ni-Zn ferrites have a relatively high resistivity, the predominant factor in P_{cv} is P_h when the ferrites are worked at relatively low frequencies[15]. With increasing MnO_2 content, average grain size gradually decreases and porosity gradually increases. Both of the grain boundaries and pores make against domain wall motion and lead to the increase of P_h. So, the sample without MnO_2, which has the biggest average grain size and the lowest porosity, obtains the lowest P_{cv}. With a further increase in frequency, the contribution of P_e in P_{cv} gradually increases and becomes the predominant factor when the excitation frequency exceeds 1 MHz. The sample with a higher resistivity favors lower P_e and P_{cv}. This fact becomes more obvious at the highest frequency. However, the sample with 2.0% MnO_2 presents a different variation at high frequency. Although it has the highest resistivity, it also obtains a higher P_{cv} than the sample with 1.6% MnO_2. This abnormal phenomenon is probably attributed to the fact that the sample has the least average grain size and the lowest sintering density, which makes against domain wall motion and rotation magnetization; furthermore, the negative influence of increasing P_h is more prominent than the positive influence of decreasing P_e. As a result, the sample with 1.6% MnO_2 has the best P_{cv} when worked at frequencies higher than 1 MHz.

4 Conclusions

1) The microstructure, sintering density, DC resistivity, permeability and power loss characteristics of the Ni-Zn ferrites are largely affected by doping MnO_2 under the specified preparation conditions. The average grain size, sintering density and permeability of the ferrite samples gradually decrease with the increase of MnO_2 content. And the DC resistivity continuously increases with increase of MnO_2 content.

2) The saturation magnetization first increases slightly, and then continuously decreases with increasing MnO_2 content. P_{cv} increases with the increase of MnO_2 content when the excitation frequency is less than 1 MHz. But it decreases with the increase of MnO_2 content when the frequency is higher than 1 MHz, except for the sample with 2.0% MnO_2. These are attributed to the fact that the predominant contribution to P_{cv} is changed from P_h to P_e with increasing frequency. And the partitioning frequency is about 1 MHz.

References

[1] MATSUO Y, INAGAKI M, TOMOZAWA T, NAKAO F. High performance NiZn ferrite [J]. IEEE Transactions on Magnetics, 2001, 37(4): 2359−2361.

[2] SU Hua, ZHANG Huai-wu, TANG Xiao-li, XIANG Xin-yuan. High-permeability and high-Curie temperature NiCuZn ferrite [J]. Journal of Magnetism and Magnetic Materials, 2004, 283(2−3): 157−163.

[3] MIRZAEE O, GOLOZAR M A, SHAFYEI A. Influence of V_2O_5 as an effective dopant on the microstructure development and magnetic properties of $Ni_{0.64}Zn_{0.36}Fe_2O_4$ soft ferrites [J]. Materials Characterization, 2008, 59(5): 638−641.

[4] SU Hua, ZHANG Huai-wu, TANG Xiao-li, JING Yu-lan. Influence of microstructure on permeability dispersion and power loss of NiZn ferrite [J]. Journal of Applied Physics, 2008, 103(9): 093903.

[5] NIU Qing-shan, JIA Hu-sheng, XU Bing-she. Current research situation and development of low-temperature sintering NiCuZn ferrite material [J]. Journal of North University of China, 2008, 29(5): 453−459. (In Chinese)

[6] DEKA S, JOY P A. Characterization of nanosized NiZn ferrite powders synthesized by an autocombustion method [J]. Materials Chemistry and Physics, 2006, 100(1): 98−101.

[7] JU Dong-ying, BIAN Pei. Low-temperature sintering method for NiCuZn ferrite and effect of Mn addition on electromagnetic properties [J]. Transactions of Nonferrous Metals Society of China, 2006, 16: s67−s70.

[8] MIRZAEE O, SHAFYEI A, GOLOZAR M A, SHOKROLLAHI A. Influence of MoO_3 and V_2O_5 co-doping on the magnetic properties and microstructure of a Ni-Zn ferrite [J]. Journal of Alloys and Compounds, 2008, 461(1−2): 312−315.

[9] TAO R B, CALTUN O, DUMITRU I. Complex permeability spectra of Ni-Zn ferrites doped with V_2O_5/Nb_2O_5 [J]. Journal of Magnetism and Magnetic Materials, 2006, 304(2): e749−e751.

[10] YUKSEL B, KIRTAY S, OZKAN T O. The effect of B_2O_3 addition to the microstructure and magnetic properties of $Ni_{0.4}Zn_{0.6}Fe_2O_4$ ferrite [J]. Journal of Magnetism and Magnetic Materials, 2008, 320(5): 714−718.

[11] LI Z W, KONG L B, YANG Z H. Study of matching characteristics for $Ni_{0.97-x}Zn_xCo_{0.03}Fe_2O_4$ spinel ferrites [J]. Journal of Applied Physics, 2009, 105(11): 113912.

[12] SINGH A K, GOEL T C, MENDIRATTA R G, THAKUR O P. PRAKASH C. Magnetic properties of Mn-substituted Ni-Zn ferrites [J]. Journal of Applied Physics, 2002, 92(7): 3872−3874.

[13] REZLESCU E, SACHELARIE L, POPA P D, REZLESCU N. Effect of substitution of divalent ions on the electrical and magnetic properties of Ni-Zn-Me ferrites [J]. IEEE Transactions on Magnetics, 2000, 36(6): 3962−3967.

[14] CEDIGHIAN S. Ferrites [M]. Bucharest: Editura Tehnica Press, 1966: 78−85.

[15] KONDO K, CHIBA T, YAMADA S. Effect of microstructure on magnetic properties of Ni-Zn ferrites [J]. Journal of Magnetism and Magnetic Materials, 2003, 254−255: 541−543.

MnO_2 掺杂 Ni-Zn 铁氧体的微观结构及磁性能

苏　桦，张怀武，唐晓莉，荆玉兰

电子科技大学 电子薄膜与集成器件国家重点实验室，成都 610054

摘　要：为了改善 Ni-Zn 铁氧体材料的功率损耗特性，基于固相反应烧结法研究 MnO_2 掺杂对 Ni-Zn 铁氧体综合性能的影响。研究发现，在 0~2.0%(质量分数)掺杂范围内，MnO_2 不会影响铁氧体的单相结构。而 Ni-Zn 铁氧体的平均晶粒尺寸、烧结密度以及磁导率都随着 MnO_2 掺杂量的增加而逐渐下降，同时，铁氧体的电阻率持续上升。饱和磁化强度(单位质量产生的磁矩)先随着 0.4% MnO_2 的掺入略有上升，而后随着 MnO_2 掺杂量的增加持续下降，这主要是受金属离子占位及超交换作用力变化的影响。当测试频率低于 1 MHz 时，铁氧体的功耗(P_{cv})随着 MnO_2 掺杂量的增加持续上升，而当测试频率超过 1 MHz 后，涡流损耗在总损耗中逐渐占主导地位，电阻率越高的样品越有利于获得低功耗，但这一规律对于 2.0% MnO_2 掺杂的样品不适用。总体而言，当频率低于 1 MHz 时，不掺杂 MnO_2 的 Ni-Zn 铁氧样品能够获得更低的功耗；而当频率超过 1 MHz 后，掺杂 1.6% MnO_2 的 Ni-Zn 铁氧体能够获得最低的功耗。

关键词：Ni-Zn 铁氧体；MnO_2；掺杂；磁性能

(Edited by YANG Hua)